

Structures and Properties of Organic Liquids: *n*-Butane and 1,2-Dichloroethane and Their Conformational Equilibria¹William L. Jorgensen,*² Robert C. Binning, Jr., and Bernard Bigot*Contribution from the Department of Chemistry, Purdue University, West Lafayette, Indiana 47907. Received October 24, 1980*

Abstract: Monte Carlo statistical mechanics simulations have been carried out for liquid *n*-butane at its boiling point and for liquid 1,2-dichloroethane (DCE) at 25 °C. The intermolecular interactions were described by Coulomb and Lennard-Jones terms in the TIPS format. The internal rotation about the central bonds in the monomers was also included by using the revised Scott-Scheraga potential for *n*-butane and a function derived from experimental data for DCE. Detailed analyses of the structures, thermodynamics, and conformational properties of the liquids are presented. The experimentally observed increase in the gauche/trans ratio for DCE in going from the gas phase to the liquid is mirrored in the computed results. However, essentially no solvent effect is found on the conformational populations for *n*-butane at the normal liquid density. The dominance of electrostatics in producing the solvent shift for DCE is proved via a simulation with the Coulombic interactions deleted. The structures of the liquids are generally similar except the CH₂...Cl pairs are better correlated in DCE than the CH₂...CH₃ pairs in *n*-butane. No repeating polymeric units are clearly evident in the liquids; the number of nearest neighbors for *n*-butane and DCE monomers in the liquids are ca. 12 and 14, respectively. Overall, the excellent agreement between the computed and experimental thermodynamic properties and conformational data confirms the capabilities of the TIPS-based statistical mechanics approach for investigating organic liquids.

Solvent effects play an important and often dominant role in determining reaction rates and such fundamental molecular properties as conformations, relative acidities, basicities, and nucleophilicities.³ Although a knowledge of structure normally precedes understanding reactivity, little detailed experimental data are available on the structures of fluids due to the complexities associated with the combined high density and relative disorder. This is in sharp contrast to the wealth of structural data on gases and solids; however, most experimental organic chemistry is performed in solution and the most widely used organic chemicals are liquids under standard conditions. Thus, it is apparent that to deepen the understanding of organic chemistry and thereby enhance the predictive abilities of organic chemists, it is essential to obtain a much greater knowledge of solvation and the structure of liquids at the molecular level.

In recent years a promising approach to studying fluids has been evolving in computer simulation techniques. Specifically, the powerful methods of molecular dynamics and Monte Carlo statistical mechanics are being applied successfully to progressively more complex fluids. The resultant structural, thermodynamic, and dynamic details have provided intimate descriptions of a variety of pure liquids and solutions including water,^{4,5} ammonia,⁶ methanol,^{5,7} ethanol,⁵ *n*-alkanes,^{8,9} methane in water,¹⁰ *n*-butane

in CCl₄,¹¹ and a dipeptide in water.¹² In addition to the demands on computational resources, a key problem in the theoretical work has been the need for intermolecular potential functions which accurately describe interactions between molecules in the fluids. Traditionally, the functions have been obtained either empirically by fitting to known properties of dimers and the liquids or by fitting to dimerization energies computed from ab initio molecular orbital calculations. The empirical approach is hindered by the shortage of accurate structural and energetic data on gas-phase dimers, while iteratively fitting to liquid-phase data is laborious. On the other hand, the quantum mechanical route is restricted by the increasing importance of dispersion effects as the monomers become larger and more polarizable. This necessitates post-Hartree-Fock calculations that are currently impractical for all but the smallest dimers.^{5,7}

A significant development has been the recent creation of transferable intermolecular potential functions (TIPS) for water, alkanes, alcohols, and ethers.⁵ The necessary parameters were obtained from several sources including earlier work on liquid alkanes and by fitting ab initio results for water, alcohol, and ether dimers and Monte Carlo results for liquid water. Monte Carlo simulations of liquid water, methanol, and ethanol based on the TIPS were then shown to yield structural and thermodynamic data in good agreement with experiment.⁵ To further investigate the TIPS approach and the structures and properties of organic liquids, we report Monte Carlo simulations of liquid *n*-butane and 1,2-dichloroethane (DCE) here.

A key focus of the work is the effects of the condensed phase on the conformational preferences of the monomers. This topic has been extensively investigated for 1,2-dihaloethanes including DCE with diffraction and spectroscopic methods.^{3f} The increased gauche/trans ratios for 1,2-dihaloethanes in polar solvents are usually explained by classical electrostatics; the gauche rotamers have large dipole moments which lead to preferential dielectric and dipole-dipole stabilization in the condensed phases. Previously internal rotation has been studied with molecular dynamics for liquid *n*-butane,^{8,9a} *n*-octane,^{9b} *n*-decane,⁸ and *n*-butane in CCl₄¹¹ and in Monte Carlo simulations of methanol and ethanol.⁵ The

(1) Quantum and statistical mechanical studies of liquids, 16. A preliminary report of this work has been made: Jorgensen, W. L. *J. Am. Chem. Soc.* **1981**, *103*, 677.

(2) Camille and Henry Dreyfus Foundation Teacher-Scholar, 1978-1983. Alfred P. Sloan Foundation Fellow, 1979-1981.

(3) Some key references are as follows: (a) Parker, A. *J. Chem. Rev.* **1969**, *69*, 1. (b) Kebarle, P. *Annu. Rev. Phys. Chem.* **1977**, *28*, 445. (c) Bartmess, J. E.; Scott, J. A.; McIver, R. T. *J. Am. Chem. Soc.* **1979**, *101*, 6046, 6056. (d) Taft, R. W. In "Kinetics of Ion-Molecule Reactions"; Ausloos, P., Ed.; Plenum Press: New York, 1979; p 271. (e) Olmstead, W. N.; Brauman, J. I. *J. Am. Chem. Soc.* **1977**, *99*, 4219. (f) Abraham, R. J.; Bretschneider, E. In "Internal Rotation in Molecules"; Orville-Thomas, W. J., Ed.; Wiley: London, 1974; Chapter 13.

(4) (a) Stillinger, F. H.; Rahman, A. *J. Chem. Phys.* **1974**, *60*, 1545. (b) Lie, G. C.; Clementi, E.; Yoshimine, M. *Ibid.* **1976**, *64*, 2314. (c) Swaminathan, S.; Beveridge, D. L. *J. Am. Chem. Soc.* **1977**, *99*, 8392. (d) Jorgensen, W. L. *Ibid.* **1979**, *100*, 2011, 2016. (e) Jorgensen, W. L. *Chem. Phys. Lett.* **1980**, *70*, 326.

(5) Jorgensen, W. L. *J. Am. Chem. Soc.* **1981**, *103*, 335, 341, 345.

(6) (a) Klein, M. L.; McDonald, I. R.; Righini, R. *J. Chem. Phys.* **1979**, *71*, 3673. (b) McDonald, I. R.; Klein, M. L. *Discuss. Faraday Soc.* **1978**, *66*, 48. (c) Jorgensen, W. L.; Ibrahim, M. *J. Am. Chem. Soc.* **1980**, *102*, 3309.

(7) Jorgensen, W. L. *J. Am. Chem. Soc.* **1980**, *102*, 543.

(8) Ryckaert, J.-P.; Bellemans, A. *Discuss. Faraday Soc.* **1978**, *66*, 95.

(9) (a) Weber, T. A. *J. Chem. Phys.* **1978**, *69*, 2347. (b) Weber, T. A. *Ibid.* **1979**, *70*, 4277.

(10) Owicki, J. C.; Scheraga, H. A. *J. Am. Chem. Soc.* **1977**, *99*, 7413. Swaminathan, S.; Harrison, S. W.; Beveridge, D. L. *Ibid.* **1978**, *100*, 5705.

(11) Rebertus, D. W.; Berne, B. J.; Chandler, D. *J. Chem. Phys.* **1979**, *70*, 3395.

(12) Rossky, P. J.; Karplus, M. *J. Am. Chem. Soc.* **1979**, *101*, 1913.

simulation of DCE is particularly significant because reliable, quantitative experimental data are available for comparison with the computed conformational results.

The Monte Carlo simulation of *n*-butane is also important due to the great interest in the conformational preferences of *n*-alkanes as models for polymers.¹³ Furthermore, there appears to be disagreement between the earlier theoretical investigations. The results of one molecular dynamics study⁸ and an approximate treatment¹⁴ have been interpreted as predicting a significant increase in the gauche population in the liquid relative to the ideal gas,^{8,9,14-16} while more extensive molecular dynamics calculations do not find a substantial shift near the normal liquid density.^{9a} This issue needs resolution since *n*-butane is a prototype system and because the information is required for other theoretical work, particularly stochastic dynamics.¹⁶

Detailed structural and thermodynamic results have also been obtained for the liquids including radial distribution functions and neighbor and energy distributions as discussed below. Overall, the excellent agreement between the computed and experimental thermodynamic data and conformer populations establishes the TIPS-based approach as an important means for elucidating the structures and properties of organic liquids at the molecular level.

Statistical Mechanics of Liquids

(a) Background. Since the computations are not commonplace, a short review is appropriate. From classical statistical mechanics, the average energy of an ensemble of simple particles such as noble-gas atoms at constant temperature and volume is expressed by eq 1. The kinetic energy term, $E_k(3/2Nk_B T)$, is separable

$$\langle E \rangle = E_k + \int E(R)P(R) dR \quad (1)$$

$$P(R) = \exp(-\beta E(R)) / \int \exp(-\beta E(R)) dR$$

$$\beta = 1/k_B T$$

from the configurational integral which represents the contributions from the interatomic interactions. The latter term is an integral over all possible geometric configurations for the ensemble (R) of the potential energy of a configuration times the probability of its occurrence expressed by the Boltzmann factor, $P(R)$. In general, the average value of a property Q can be given analogously by eq 2. The key problem is then how to solve such configura-

$$\langle Q \rangle = Q_k + \int Q(R)P(R) dR \quad (2)$$

tional integrals. A viable solution was provided in the classic paper by Metropolis et al.¹⁷ First, they introduced periodic boundary conditions which lead to simulating a liquid by explicitly considering only a relatively small number of atoms or molecules, ca. 50–1000. Typically a cubic sample is employed which is surrounded by images of itself. If on moving a particle to create a new configuration it passes through a wall, then an image of it reenters the central cube through the opposite face. Secondly, Metropolis et al. devised a procedure for picking configurations such that they occur with a probability equal for their Boltzmann factor. This speeds convergence by avoiding excessive sampling of high-energy configurations which contribute little to the integrals. Using Metropolis sampling and changing the integral in eq 2 to a sum over configurations yields eq 3 where R' indicates

$$\langle Q \rangle = Q_k + \frac{1}{M} \sum_i^M Q_i(R') \quad (3)$$

a Metropolis selected configuration. Convergence of the energy

(13) For key references, see: (a) Flory, P. J. "Statistical Mechanics of Chain Molecules"; Wiley-Interscience: New York, 1969. (b) Dettenmaier, M. *J. Chem. Phys.* **1978**, *68*, 2319.

(14) Pratt, L. R.; Hsu, C. S.; Chandler, D. *J. Chem. Phys.* **1978**, *68*, 4202.

(15) Chandler, D. *Discuss. Faraday Soc.* **1978**, *66*, 184.

(16) Levy, R. M.; Karplus, M.; McCammon, J. A. *Chem. Phys. Lett.* **1979**, *65*, 4.

(17) Metropolis, N.; Rosenbluth, A. W.; Rosenbluth, M. N.; Teller, A. H.; Teller, E. *J. Chem. Phys.* **1953**, *21*, 1087.

Table I. TIPS Parameters for *n*-Butane and DCE^a

site	q	$10^{-4} A^2$	C^2
<i>n</i> -butane			
CH ₂	0.0	729	1825
CH ₃	0.0	795	2400
DCE			
CH ₂	0.25	729	1825
Cl	-0.25	600	2600

^a Units are for q (electrons), A^2 ((kcal Å¹²)/mol) and C^2 ((kcal Å⁶)/mol). e^2 in eq 7 is 332.17752 (kcal Å)/mol.

is usually obtained in liquid simulations within ca. 500 000 (500K) configurations; however, convergence must be established for each computed quantity. The initial configurations needed to reach equilibrium are discarded and final averaging is performed over an additional ca. 500–1000K configurations.

In our simulations of molecular liquids, the sampling has included internal rotational degrees of freedom, but not vibrations in the monomers. Thus, eq 4 is assumed in which the vibrational

$$\langle Q \rangle = Q_k + Q_v + \frac{1}{M} \sum_i Q_i(R') \quad (4)$$

contribution, Q_v , is decoupled from the configurational integral, which is clearly an approximation.

A critical item is the energy of a configuration which is obtained from the pairwise sum of the dimerization energies between all monomers (eq 5). This is required because a Boltzmann term

$$E_i = \sum_{a<b} \Delta E_{ab} \quad (5)$$

appears in the Metropolis sampling algorithm and in order to calculate various energetic properties. Higher order terms such as three-body contributions could also be considered, however, including them in a simulation is arduous and their form is not well established. Three-body effects are likely most important in hydrogen-bonded liquids due to the highly polar nature of the interactions and the relatively short intermolecular distances. From many theoretical studies it has consistently been found that three-body effects are constructive and account for ca. 15% of the intermolecular energy in hydrogen bonded liquids.⁴⁻⁷ Their influence in other solvents appears much diminished as discussed below.

A spherical cutoff is normally assumed in evaluating the dimer interactions. For interactions with more than one image of a monomer to be avoided, the maximum cutoff is at an intermolecular separation equal to half the length of an edge of the periodic cube. The number of monomers and therefore the volume of the cube should be large enough so that the results are essentially unaffected by increasing the system size. For polarizable monomers, a cutoff correction to the energy should be made via eq

$$E_{\text{corr}} = 2\pi\rho_y \int_{r_c}^{\infty} r^2 g_{xy}(r) u_{xy}(r) dr \quad (6)$$

6 for each pair of interacting particles (x, y) where ρ_y is the density of particles of type y (N_y/V), $u(r)$ is the interaction potential and $g_{xy}(r)$, the xy radial distribution function, is assumed to be 1 beyond the cutoff, r_c .

Thus, the principal element in the statistical mechanical treatment of liquids is the intermolecular potential functions. Their choice for the present simulations is described in the next section. Incidentally, these calculations are referred to as "Monte Carlo" because some random numbers are used in generating the configurations; however, the choice of configurations is not random in view of the Metropolis sampling. A better name would be Metropolis calculations.

(b) Potential Functions. The intermolecular potential functions were represented in the TIPS format.⁵ The monomers each contain four interaction sites: for *n*-butane, the methylene and methyl groups, and for DCE, the methylenes and chlorine atoms. The sites interact intermolecularly via Coulomb and Lennard-

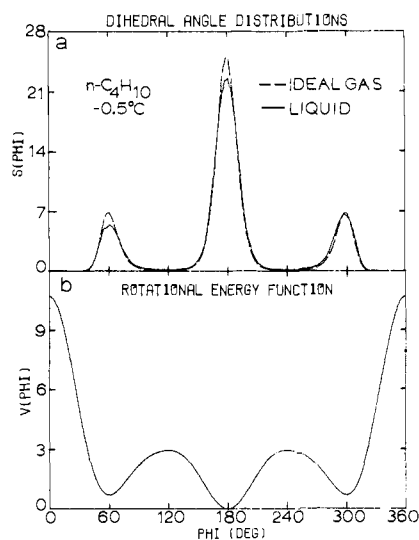


Figure 1. (a) Computed population distributions for the dihedral angle about the central CC bond in *n*-butane. Units for $s(\phi)$ are mole fraction per degree $\times 10^{-3}$. (b) Potential function (kcal/mol) for rotation about the central CC bond in *n*-butane.

Jones terms (eq 7). The A and C parameters for hydrocarbon groups were previously reported⁵ and remained unchanged in this work as summarized in Table I.

$$\Delta E_{ab} = \sum_i \sum_j \left(\frac{q_i q_j e^2}{r_{ij}} + \frac{A_i A_j}{r_{ij}^{12}} - \frac{C_i C_j}{r_{ij}^6} \right) \quad (7)$$

The parameters for chlorine were chosen to yield reasonable (1) liquid-phase dipole moments for alkyl chlorides and (2) gas-phase geometries and dimerization energies for HCl and Cl₂ dimers in comparison with ab initio calculations.^{18,19} The resultant TIPS parameters are also shown in Table I. The charge of -0.25 electron for chlorine requires assignment of +0.25 to methylene in DCE to preserve neutrality, while there are no Coulombic terms for the intermolecular interactions of *n*-butane molecules. Standard geometries were employed for the monomers that are consistent with earlier work⁸ and diffraction data:²⁰ $r(\text{CC}) = 1.530 \text{ \AA}$, $r(\text{CCl}) = 1.785 \text{ \AA}$, $\angle \text{CCC} = \angle \text{CCCl} = 109.47^\circ$.

The TIPS parameters for chlorine provide the following results for reference systems. The dipole moment of methyl chloride (2.14 D) is greater than the experimental gas-phase value (1.87 D) which is necessary to reflect increased polarization in the condensed phase.⁵ The Cl-Cl distance and dimerization energy for linear HCl dimer are 3.69 Å and -1.61 kcal/mol; the 4-31G calculations of Kern and Allen predict 3.99 Å and -2.10 kcal/mol.¹⁸ The corresponding TIPS results for the linear Cl₂ dimer are 4.0 Å and -0.39 kcal/mol, while ab initio computations including dispersion yield 3.45 Å and -0.51 kcal/mol.¹⁹ In view of the uncertainties in the ab initio data and the fact that the TIPS parameters need to correspond to the liquid state and not the gas, the results are reasonable.

The last component is the potential functions for internal rotation about the central CC bonds in the monomers, $V(\phi)$. For *n*-butane, the revised Scott-Scheraga potential was adopted from the earlier molecular dynamics study.⁸ It is given in eq 8 and

$$V(\phi) = 2.218 - 2.905 \cos \phi - 3.136 \cos^2 \phi + 0.731 \cos^3 \phi + 6.272 \cos^4 \phi + 7.527 \cos^5 \phi \quad (8)$$

plotted in Figure 1b. The trans and gauche minima are at 180° and ±60° with gauche 0.70 kcal/mol above trans. The cis

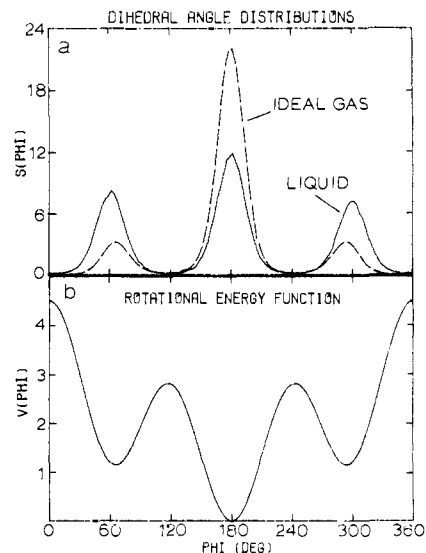


Figure 2. (a) Computed population distributions for the dihedral angle about the CC bond in DCE. Units for $s(\phi)$ are mole fraction per degree $\times 10^{-3}$. (b) Potential function (kcal/mol) for rotation about the CC bond in DCE.

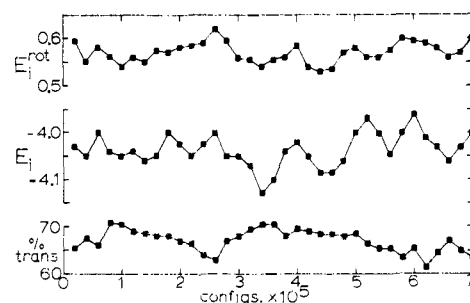


Figure 3. Average total and internal rotational energies (kcal/mol) and trans populations for each increment of 20K configurations during the final averaging in the Monte Carlo simulation of liquid *n*-butane.

maximum is at 10.7 kcal/mol, and the trans to gauche barrier height is 2.95 kcal/mol.

For DCE, a function given by the Fourier expansion in eq 9 $V(\phi) = 1/2V_1(1 + \cos \phi) + 1/2V_2(1 - \cos 2\theta) + 1/2V_3(1 \cos 3\theta)$ (9)

was derived that fits the available gas-phase experimental data on the barrier heights and trans/gauche energy difference.²⁰⁻²² V_1 , V_2 , and V_3 are 1.933, -0.333, and 2.567 which give the gauche minima at ±66° and 1.14 kcal/mol above trans as illustrated in Figure 2b. The cis maximum is at 4.50 kcal/mol, and the trans to gauche barrier height is 2.81 kcal/mol. The chief differences in the two functions are the lower gauche to trans and gauche to gauche barriers for DCE than *n*-butane.

(c) **Liquid Simulations.** The Monte Carlo calculations were executed by using cubic samples of 128 monomers, periodic boundary conditions, and Metropolis sampling. The simulations were run for *n*-butane at its boiling point (-0.5 °C) and at 25 °C for DCE with the corresponding experimental densities, 0.602 and 1.246 g cm⁻³.^{23,24} Spherical cutoffs at 11 Å were invoked in evaluating the TIPS which includes interactions with a monomer's ca. 40 nearest neighbors. New configurations were generated

(21) Lowe, J. P. *Prog. Phys. Org. Chem.* **1968**, *6*, 1.

(22) Tanabe, K. *Spectrochim. Acta, Part A* **1972**, *28A*, 407.

(23) (a) Rossini, F. D.; Pitzer, K. S.; Arnett, R. L.; Brown, R. M.; Pimentel, G. C. "Selected Values of Physical and Thermodynamic Properties of Hydrocarbons and Related Compounds"; American Petroleum Institute; Carnegie Press: Pittsburgh, 1953. (b) Aston, J. G.; Messerly, G. H. *J. Am. Chem. Soc.* **1940**, *62*, 1917. (c) Chen, S. S.; Wilhoit, R. C.; Zwolinski, B. J. *J. Phys. Chem. Ref. Data* **1975**, *4*, 859.

(24) Wilhelm, E.; Schano, R.; Becker, G.; Findenegg, G. H.; Kohler, F. *Trans. Faraday Soc.* **1969**, *65*, 1443.

(18) Kerns, R. C.; Allen, L. C. *J. Am. Chem. Soc.* **1978**, *100*, 6587.

(19) Prissette, J.; Kochanski, E. *J. Am. Chem. Soc.* **1978**, *100*, 6609.

(20) Kveseth, A. *Acta Chem. Scand., Ser. A* **1975**, *A29*, 307.

by randomly selecting a monomer, translating it in all three Cartesian directions, rotating it about one axis, and performing the internal rotation. For *n*-butane an acceptance rate of 44% was maintained by using ranges of ± 0.15 Å, $\pm 15^\circ$, and $\pm 20^\circ$ for the motions, respectively. The acceptance rate and ranges for DCE were 41%, ± 0.12 Å, $\pm 12^\circ$, and $\pm 15^\circ$. The smaller ranges for DCE are likely a consequence of the 18% lower molar volume for DCE (131.9 Å³/molecule) than *n*-butane (160.4 Å³/molecule).

A particular concern for these calculations is that they are run long enough to obtain convergence of the trans and gauche populations. This was firmly established for *n*-butane by making two runs with the monomers initially all cis and initially all trans. The two calculations required 800K configurations each to converge to the same total and internal energies and conformer populations. Final averaging occurred for one run over an additional 700K configurations. The fluctuations in the energies and populations during the last segment are shown in Figure 3. No drift in the averages of these quantities is apparent. Convergence was also supported by monitoring the barrier crossings during the final 200K configurations. There were 118 gauche to trans and 122 trans to gauche conversions during this segment. Therefore, the total number of *barrier crossings* during the run was ca. 1800; however, most of the crossings are futile with the molecule soon returning to its initial conformational state. From analysis of the results it can be estimated that one in five crossings yield a true transition such that the molecule stays in and explores the new state for an extended period. Thus, the total number of *transitions* during the run was ca. 360 with ca. 170 occurring during the averaging. These numbers can be compared with the earlier molecular dynamics results; Ryckaert and Bellemans⁸ found 88 transitions for 64 molecules during their 14-ps run at 292 K and Weber's^{9a} reported transition frequency indicates 50–60 transitions for 100 molecules in 24 ps at 315 K. It should be noted that 1500K configurations represent a comparatively long Monte Carlo run and required about 20 h on a CDC/6600 computer.

For DCE, the initial configuration was derived from one in the simulations of *n*-butane. The total and internal energies and conformer populations were fully equilibrated in 700K configurations. An additional 405K configurations were used for averaging. The totals for barrier crossings during the averaging also confirmed the equilibrium: 194 gauche to trans, 193 trans to gauche, 81 gauche⁺ to gauche⁻, and 79 gauche⁻ to gauche⁺. Gauche to gauche transitions did not occur in the simulation of liquid *n*-butane due to the lower temperature and higher barrier (10.0 vs. 3.4 kcal/mol). For a test of the influence of the electrostatics, a simulation of liquid DCE was also executed with the Coulombic terms deleted. All other conditions and parameters were unchanged. Starting from a configuration of the earlier simulation, 560K configurations were required for equilibration and an additional 315K were used for averaging in this case.

Results and Discussion

(a) Thermodynamics. The intermolecular potential energy, E_i^{inter} , the intramolecular rotational energy, E_i^{rot} , and the contribution to the heat capacity due to fluctuations in E_i^{inter} , C_V^{inter} , are computed directly in the simulations. Cutoff corrections for E_i^{inter} were evaluated via eq 6 for the Lennard-Jones terms in the potentials and amounted to -0.33 kcal/mol for *n*-butane and -0.42 for DCE. The corrected values are reported in Table II.

For comparison with experimental data the enthalpy of vaporization, ΔH_v , and total heat capacity, C_V , may be computed as follows. The energy of vaporization for the liquid going to the ideal gas, ΔE_v° , is defined by eq 10 which becomes eq 11 by

$$\Delta E_v^\circ = E(\text{g}) - E(\text{l}) \quad (10)$$

$$\Delta E_v^\circ = E^{\text{rot}}(\text{g}) - (E_i^{\text{inter}}(\text{l}) + E_i^{\text{rot}}(\text{l})) \quad (11)$$

$$\Delta H_v^\circ = \Delta E_v^\circ + P(V^\circ(\text{g}) - V(\text{l})) \quad (12)$$

$$\Delta H_v = \Delta H_v^\circ - (H^\circ - H) \quad (13)$$

Table II. Thermodynamic Properties for Liquid *n*-Butane at -0.5 °C and DCE at 25 °C^a

property	<i>n</i> -butane	DCE
E_i^{inter}	-4.94 ± 0.02	-8.26 ± 0.02
E_i^{rot}	0.57 ± 0.01 (0.56) ^b	1.03 ± 0.01 (0.62) ^b
ΔE_v°	4.93	7.84
ΔH_v°	5.47	8.44
ΔH_v	5.39 (5.35) ^c	8.40 (8.40) ^d
C_V^{inter}	2.2 ± 0.2	4.6 ± 0.7
C_V	22.0 (23.1) ^e	21.1 (21.3) ^f

^a Energies in kcal/mol; heat capacities in cal/(mol deg). Experimental values in parentheses. ^b Ideal-gas values obtained from Boltzmann distributions for eq 8 and 9. ^c Reference 23. ^d Reference 25. ^e See text. ^f Reference 26.

assuming the same vibrational and kinetic energies for the ideal gas and liquid. The rotational energy for the ideal gas is obtained from a Boltzmann distribution for $V(\phi)$ as recorded in Table II. Then, ΔE_v° is related to ΔH_v via eq 12 and 13 where the work term in eq 12 is essentially RT in most cases and $H^\circ - H$ is the enthalpy departure function for the *real* gas. The last term can be evaluated by using the virial equation of state according to eq 14 where B is the second virial coefficient for the gas. The problem

$$H^\circ - H = \frac{RT}{V} \left(T \frac{dB}{dT} - B \right) \quad (14)$$

is then to find the necessary virial coefficient data. Fortunately, $B(T)$ has been reported for *n*-alkanes²⁷ and leads to $H^\circ - H = 0.08$ kcal/mol for *n*-butane at -0.5 °C. However, for DCE the $B(T)$ data do not appear to be available, so $B(T)$ was estimated from the Berthelot expression (eq 15) which is known to give good

$$B(T) = \frac{9RT_c}{128P_c} \left(1 - \frac{6T_c^2}{T^2} \right) \quad (15)$$

results for ethyl chloride.²⁸ The resultant $H^\circ - H$ is 0.04 kcal/mol which also agrees with the value of 0.03 kcal/mol which can be obtained from the van der Waals expression. Clearly, these corrections are small since the gases are relatively ideal. The net result is that the computed heats of vaporization are 5.39 and 8.40 kcal/mol for *n*-butane at -0.5 °C and DCE at 25 °C which agree remarkably with the experimental data, 5.35 and 8.40 kcal/mol.^{23,25}

The heat capacities of the liquids are dominated by the contributions from the kinetic and vibrational energy of the monomers. This is best approximated by the heat capacity of the ideal gas, C_V° , to which C_V^{inter} may be added to obtain an estimate of C_V for the liquid. The computed results in Table II are within 5% of the experimental values, through the minor contribution of C_V^{inter} is emphasized. Experimental values for C_V are not reported as often as for C_P . Both are available for DCE;²⁶ however, for *n*-butane the experimental C_P had to be converted via eq 16 by

$$C_P - C_V = \frac{\alpha^2 V(\text{l}) T}{\beta} \quad (16)$$

using reported data for the expansivity and compressibility of liquid alkanes.²⁹ The heat capacities for ideal gases are available in compilations.³⁰ Finally, it is noted that the standard deviations (2σ) for computed properties were calculated from separate averages over each increment of 20K configurations for *n*-butane and 15K for DCE.

(b) Internal Rotation. The computed distribution functions for the dihedral angles, $s(\phi)$, for the liquids and ideal gases are shown

(27) McGlashan, M. L.; Potter, D. J. B. *Proc. R. Soc. London, Ser. A* **1962**, *267*, 478.

(28) Lambert, J. D.; Roberts, G. A. H.; Rowlinson, J. S.; Wilkinson, V. *Proc. R. Soc. London, Ser. A* **1949**, *196*, 113.

(29) Blinowski, A.; Brostow, W. *J. Chem. Thermodyn.* **1975**, *7*, 787.

(25) Wadso, I. *Acta Chem. Scand.* **1968**, *22*, 2438.
(26) Wilhelm, E.; Grolier, J. P. E.; Ghasseni, M. H. K. *Ber. Bunsenges. Phys. Chem.* **1977**, *81*, 925.

(30) Reid, R. C.; Prausnitz, J. M.; Sherwood, T. K. "The Properties of Gases and Liquids", 3rd ed.; McGraw-Hill: New York, 1977.

Table III. Conformational Data for *n*-Butane at -0.5°C and DCE at 25°C

	computed		
	<i>n</i> -butane	DCE	exptl DCE ^a
% trans gas	67.7	76.5	77 ± 2
% trans liquid	67.1 ± 0.8	43.5 ± 0.5	35 ± 4
x_g/x_t gas	0.48	0.31	0.30 ± 0.03
x_g/x_t liquid	0.49 ± 0.02	1.30 ± 0.02	1.86 ± 0.3

^a Reference 22.

in Figures 1a and 2a. For *n*-butane the condensed phase has little effect on the distribution, while there is a dramatic increase in the gauche population in liquid DCE relative to the gas. The trans populations are calculated by integrating the distributions from 120° to 240° , the remainder being gauche. The quantitative results are given in Table III and compared to the experimental data for DCE obtained from analyses of IR intensities.²² There is no shift in populations for *n*-butane within the statistical limits of the calculations when the standard deviations are computed in the usual way from the incremental fluctuations (Figure 3). However, the slight asymmetry in Figure 1a should be noted; the average gauche⁻ and gauche⁺ populations are 15.0% and 17.9%. This implies an average of 19.2 monomers were gauche⁻ and 22.9 were gauche⁺. With small sample sizes and reasonable length runs it would be fortuitous for these populations to exactly balance. Although the equilibration studies indicated that total trans/gauche equilibrium was established, the asymmetry could possibly be used to provide error bars of ca. $\pm 3\%$ for the populations. As will be presented elsewhere in detail, we have also recently completed extensive Monte Carlo simulations of liquid *n*-butane in the NPT ensemble at -0.5°C and from 1 to 15 000 atm. Each run involved 2–3 million configurations. The computed densities with the TIPS potentials are within 3% of experiment at all pressures. Furthermore, at 1 atm the computed trans population is $67.8 \pm 1.3\%$ which is in exact accord with the present results. Consequently, it must be concluded that if there is a condensed-phase effect on the populations for *n*-butane, it must be very slight at the normal liquid density. The available experimental data are inconclusive on this point. Although for liquid *n*-butane Raman and Rayleigh scattering results concur that the ΔH for the trans to gauche conversion is 0.76 ± 0.10 kcal/mol, gas-phase values from a variety of sources range from 0.50 to 0.97 kcal/mol.^{23c}

The trans populations from the previous theoretical studies of liquid *n*-butane all scaled to 0°C are 56%⁸ and 65–68%^{9a} from the molecular dynamics calculations and 60% from the calculations of Pratt, Hsu, and Chandler.¹⁴ In view of the differences in the treatments, conditions, and potential functions, these results are in reasonable agreement with the present predictions except for the low value of Ryckaert and Bellemans. The potential functions and conditions were essentially identical in their simulation and here. Consequently, the most likely explanation is that their molecular dynamics run was not fully equilibrated; it had half the duration of Weber's simulations,^{9a} many fewer barrier crossings than the present work and far greater asymmetry in the computed $s(\phi)$.⁸

It is gratifying that the experimentally observed increase in the gauche population for liquid DCE is nicely mirrored in the computed results. The agreement for the trans populations is nearly quantitative in view of the experimental uncertainties. This and the excellent thermodynamic results are most encouraging and establish the TIPS-based Monte Carlo approach as an important means for investigating conformational problems in organic liquids. A possible further implication is that three-body effects are relatively unimportant in liquids such as alkanes and DCE in comparison to the hydrogen bonded liquids for which the TIPS-based simulations did underestimate the experimental ΔH_v 's by the anticipated ca. 15% (vide supra).⁵

It seems likely that the difference in the condensed phase effects on $s(\phi)$ for the liquids is due to the electrostatics in liquid DCE as mentioned above. Nevertheless, a packing effect^{14,15} could also

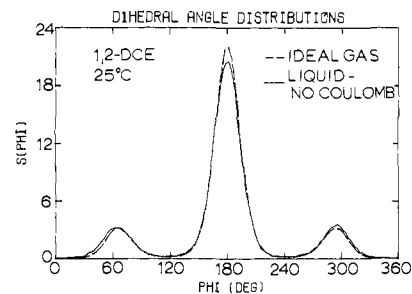


Figure 4. Computed population distributions for the dihedral angle in liquid DCE with the Coulombic terms left out (solid line) and in the ideal gas (dashed line).

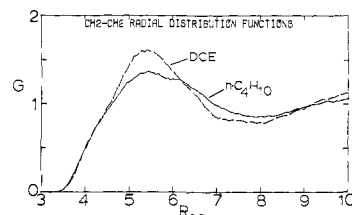


Figure 5. Computed intermolecular $\text{CH}_2\text{-CH}_2$ radial distribution functions for liquid *n*-butane and DCE. Distances are in Å throughout.

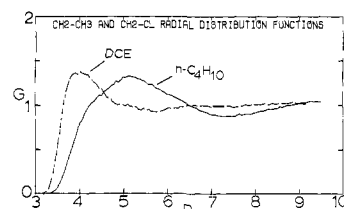


Figure 6. Computed intermolecular $\text{CH}_2\text{-CH}_3$ RDF for liquid *n*-butane and $\text{CH}_2\text{-Cl}$ RDF for liquid DCE.

be considered in view of the significantly lower molar volume for DCE. This was tested by performing the simulation for liquid DCE with the Coulombic terms left out. When the electrostatics were turned off, the dihedral angle distribution drifted back to essentially the ideal-gas results. A total of 560K configurations were needed to fully reequilibrate the system. The $s(\phi)$ obtained by averaging over an additional 315K configurations is compared to the ideal-gas distribution in Figure 4. The conclusion is clear; the added electrostatics, and not the higher density, are responsible for the increased gauche population in liquid DCE.

There has been some discussion recently concerning the effects of constraining the bond lengths and bond angles on the computed $s(\phi)$.^{31,32} As Fixman demonstrated, compensating corrections can be made to $V(\phi)$ which amounted to only "a few tenths of $k_B T$ " in his studies of polymer chains.³¹ Not surprisingly, Chandler and Berne found that including the Fixman correction in their simulation of *n*-butane in CCl_4 did not alter the gauche to trans ratio from the constrained result.³²

In closing this section, it is noted that the computed internal rotational energies in Table II are consistent with the conformational populations and their shifts discussed above.

(c) **Structure.** Radial distribution functions (RDFs) represent the deviations in the distributions of atoms in a liquid from the values expected from the bulk density. Specifically, the density of *y* atoms about atoms of type *x* is $\rho_{xy}(r) = \rho_y^\circ g_{xy}(r)$ where *r* is the *xy* separation, ρ_y° is N_y/V and $g_{xy}(r)$ is the *xy* RDF. If a liquid is structureless, then $g_{xy}(r) = 1$. Although RDFs can be determined from diffraction experiments on liquids, such data are not currently available for *n*-butane and DCE.

The corresponding RDFs from the simulations are compared in Figures 5–7. The $\text{CH}_2\text{-CH}_2$ functions in Figure 5 are similar,

(31) Fixman, M. J. *Chem. Phys.* **1978**, *69*, 1527.(32) Chandler, D.; Berne, B. J. *J. Chem. Phys.* **1979**, *71*, 5386.

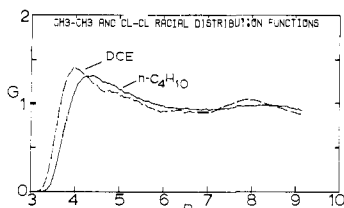


Figure 7. Computed intermolecular $\text{CH}_3\text{-CH}_3$ RDF for liquid *n*-butane and Cl-Cl RDF for liquid DCE.

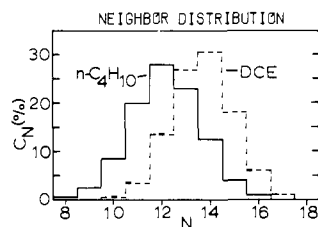


Figure 8. Computed distributions of neighbors for liquid *n*-butane and DCE. The ordinate gives the percentage of monomers with the number of neighbors shown on the abscissa.

although somewhat greater structure is implied for DCE by the sharper first peak. Both first peaks are broad and have their first minima at 7.9 Å which can be taken as an estimate of the extremity of the first shell of neighbors. Integration to this point yields an average of 12.2 neighbors for an *n*-butane monomer and 14.8 for DCE.

A more detailed breakdown for the distribution of neighbors was obtained subsequently by analyzing configurations that were saved at each interval of 2000 attempted moves. The distributions of neighbors shown in Figure 8 were obtained from defining a neighbor by a separation within 7.9 Å between the midpoints of the central CC bonds. Although the average coordination numbers are about 12 for *n*-butane and 14 for DCE, the distributions have substantial ranges, indicating a wide variety of environments for a monomer. The higher coordination number for DCE is attributable to the higher density and more attractive intermolecular interactions in the first shell as discussed further below.

Other analyses were performed to compare the environments for gauche and trans monomers in the liquids. It was found that both conformers have the same average total coordination numbers. Furthermore, the average numbers of gauche and trans neighbors were essentially the same for both conformers in the liquids. Thus, no differential effects such as gauche monomers preferring gauche neighbors were apparent.

Returning to the RDFs, the major difference in Figures 5–7 occurs in comparing the $\text{CH}_2\text{-CH}_3$ RDF for *n*-butane with $\text{CH}_2\text{-Cl}$ for DCE (Figure 6). The first peak is sharper for DCE and shifted to shorter separation by 1 Å, which is significantly greater than the difference in van der Waals radii for a methyl group and chlorine, ca. 0.2 Å. The stronger correlation of the methylene and chlorine positions is readily attributed to the added Coulombic attraction between the groups. This is supported by the comparatively small shift for the Cl-Cl first peak in Figure 7 which is roughly consistent with the difference in van der Waals radii.

For the structures of the liquids to be further elucidated, stereoplots of configurations from the simulations can be analyzed. Examples for liquid *n*-butane and DCE are presented in Figures 9 and 10. In view of the periodicity, it should be recalled that molecules near one face interact with molecules near the opposite face. Also, the cube in the drawings is actually somewhat (ca. 1 Å) outside the limits of the periodic cube. There is much disorder in both liquids with no repeating polymeric units evident. This contrasts the polymeric chains and rings found in the hydrogen bonded liquids.^{4e,5,6c,7} The bonding in the present liquids is clearly much more dominated by dispersion forces which are relatively nondirectional and, therefore, lead to little distinct structure.

The higher incidence of gauche monomers for DCE is apparent in comparing the stereoplots. Furthermore, there seems to be a definite tendency to maximize the $\text{CH}_2\text{-Cl}$ interactions between neighbors. The advantage of an increase in gauche monomers in this sense is that a neighboring chlorine can interact in a unobstructed way with both methylene groups on a gauche monomer. A head-to-tail alignment of the dipoles of neighboring gauche monomers is not indicated or supported by the neighbor analyses described above. In fact, it appears rare from the stereoplots that both chlorines from one monomer are similarly

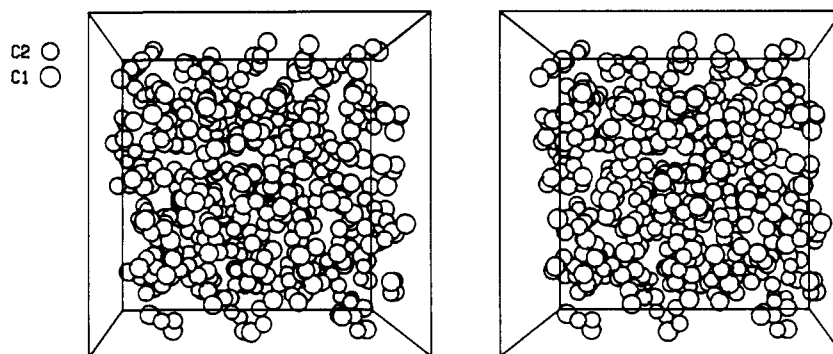


Figure 9. Stereplot of a configuration from the simulation of liquid *n*-butane. The periodic cube contains 128 monomers.

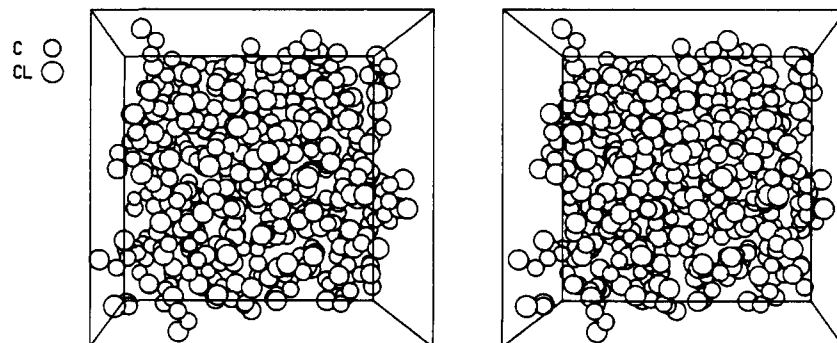


Figure 10. Stereplot of a configuration from the simulation of liquid DCE. The periodic cube contains 128 monomers.

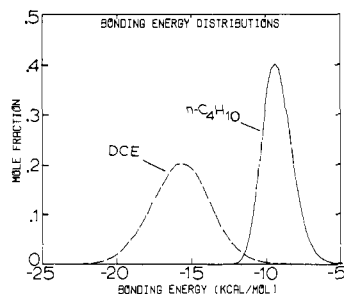


Figure 11. Computed distributions of intermolecular bonding energies for monomers in liquid *n*-butane and DCE. The units for the ordinate are mole fraction per kcal/mol.

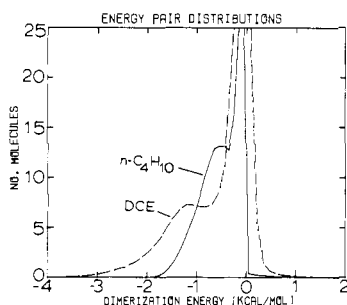


Figure 12. Computed distributions of dimerization energies for a monomer in liquid *n*-butane and DCE. The units for the ordinate are molecules per kcal/mol.

proximate to a methylene group in the same neighbor.

Thus, the picture that emerges is one of substantial disorder for both liquids, coordination numbers of 12 to 14, little total dipole alignment in DCE, but a tendency to maximize $\text{CH}_2\text{-Cl}$ interactions. One final structural point worth noting from Figure 2 is that the average dihedral angle for the gauche conformer in DCE shifts from $\pm 66^\circ$ to $\pm 61^\circ$ in going from the gas to the liquid. This effect is also consistent with simple electrostatic³³ and steric considerations. Namely, the dipole moment increases and the hindrance of the $\text{CH}_2\text{-Cl}$ intermolecular interactions decreases as ϕ approaches 0° .

(d) Energy Distributions. The energetic environments of the monomers in the liquids can also be monitored during the simulations. The distributions of total intermolecular bonding energies for monomers are shown in Figure 11. The monomers experience an energetic continuum of environments covering ranges of ca. 7

kcal/mol for *n*-butane and 10 kcal/mol for DCE. The larger range and broader peak for DCE are due to the higher temperature and to the greater variety of interactions permitted by the Coulomb terms. Similar unimodal plots have been obtained for the hydrogen bonded liquids, through the curves are not always so symmetrical and the ranges are twice as great since monomers may be in 0–4 hydrogen bonds.^{4d,e,5,6c,7}

The distributions of dimerization energies that a monomer experiences on the average are given in Figure 12. The ordinate records the average number of molecules that are bound to a monomer with the dimerization energy shown on the abscissa. The broader range of interactions for DCE is again due to the added electrostatics. The spikes near 0 kcal/mol are caused by the many molecules in the bulk that are far from the reference monomer, while the shoulders at low energy are assigned to the near neighbors. Integration of the shoulders yields estimates of coordination numbers of about 12 for both *n*-butane and DCE which is consistent with the previous values from the RDFS in view of the uncertainties in the integration limits.

The effect of the electrostatics in DCE is evident; a wider range of interactions is permitted which allows stronger attraction between near neighbors and leads to a lower overall energy and consequently higher heat of vaporization.

Conclusion

The present study demonstrates that it is possible to theoretically model complex organic liquids and obtain detailed insights into their structures and even conformational characteristics at the molecular level. For 1,2-dichloroethane, it was established that the increased gauche population in the liquid relative to the ideal-gas results from the drive to maximum the intermolecular Coulombic attractions between the methylenes and chlorine atoms. Packing effects associated with the lower molecular volume for DCE are not influential in this regard at the normal liquid density. Consistently, the conformational populations for nonpolar *n*-butane were found to be essentially the same for the ideal gas and the liquid at the normal density. The importance of such investigations stems from the profound role and limited understanding of solvation and solvent effects in organic chemistry. The TIPS-based approach appears particularly promising in view of the simple form and transferability of the potential functions. Applications and extensions to other pure liquids and dilute solutions are in progress.

Acknowledgment. Gratitude is expressed to the National Science Foundation (Grant CHE7819446) for financial assistance. Acknowledgment is also made to the donors of the Petroleum Research Fund, administered by the American Chemical Society, for partial support of this work. Discussions with Professor D. Chandler and use of Mr. Phillip Cheeseman's stereoplotting program were also greatly appreciated.

(33) LeFevre, R. J. W.; Ritchie, G. L. D.; Stiles, P. J. *J. Chem. Soc., Chem. Commun.* **1966**, 846.